Nanoscale

COMMUNICATION

Silicon nanoparticles as Raman scattering enhancers†

Cite this: *Nanoscale*, 2014, **6**, 5666

Received 30th January 2014
Accepted 21st March 2014

DOI: 10.1039/c4nr00593g

www.rsc.org/nanoscale

I. Rodriguez,[ab] L. Shi,[ab] X. Lu,[c] B. A. Korgel,[c] R. A. Alvarez-Puebla*[de] and F. Meseguer*[ab]

In this communication we demonstrate the large amplification values of the Raman signal of organic molecules attached to silicon nanoparticles (SiNPs). Light induced Mie resonances of high refractive index particles generate strong evanescent electromagnetic (EM) fields, thus boosting the Raman signal of species attached to the nanoparticles. The interest of this process is justified by the wide range of experimental configurations that can be implemented including photonic crystals, the sharp spectral resonances easily tuneable with the particle size, the biocompatibility and biodegradability of silicon, and the possibility of direct analysis of molecules that do not contain functional groups with high affinity for gold and silver. Additionally, silicon nanoparticles present stronger field enhancement due to Mie resonances at larger sizes than gold.

Metallic nanostructures and nanoparticles have attracted great attention in the last few years as they have opened up new fields of research as metamaterials.[1–3] The dramatic amplification of the Raman signal of organic species in close proximity to plasmonic nanoparticles, known as surface-enhanced Raman scattering,[4,5] is widely used as a versatile analytical technique because of its multiplex capacity, possibility of remote sensing and ultrasensitive detection.[6,7] Nanoparticles of coinable metals show strong light scattering properties produced by the collective oscillations of their surface electrons (localized surface plasmon resonances, LSPR),[8,9] generating a huge evanescent electric field near the particle surfaces. As the Raman signal is proportional to the fourth power of the local electric field at the metal nanoparticle, the Raman amplification reaches values of up to 10^{10} in non-resonant molecules,[10] giving rise to detection limits up to the single molecule level.[11,12] Although gold and silver are the most common plasmonic metals, the concept of SERS has been extended to other nanomaterials like aluminum particles,[13] metal chalcogenides (including oxides, sulfides, selenides and tellurides)[14,15] or doped semiconductors with the capability of tuning the plasmon frequency through the dopant concentration.[16] Although SERS is considered to be a purely electromagnetic effect in nature, with contributions due to charge transfer, surface-assisted Raman amplification has been demonstrated with other materials such as quantum dots,[17] or graphene.[18–20] In these cases, the SERS enhancement has been modest and can be attributed exclusively to chemical effects (*i.e.* the resonant Raman effect induced by the optical transitions between electronic levels).

Large optical fields are, however, not exclusive of metallic particles. For example, large enhancement of the Raman cross-section has been predicted in Bloch surface waves of fully dielectric structures.[21,22] Further, high electrical fields can also be attained with micro- and nanostructures.[23] In such materials, the strong scattering properties do not originate from collective excitations of electrons in the metal particle, but from the optical resonances of the whispering gallery modes (WGMs), also called Mie resonances, of nanostructures.[24,25] As a consequence of the large scattering cross-section values, the Raman signal, of any specie either inside the cavities[26–29] or attached to them,[30–33] is dramatically enhanced, thus being termed silicon particle enhanced Raman scattering (SiPERS).[28] Therefore, high refractive index nanostructures like silicon nanoparticles would also present huge fields not only inside the particles but also around them thus allowing their use as SiPERS enhancers. However, although theory predicts very large Raman signal enhancement factors with similar values to those appearing for noble metals,[30] to the best of our knowledge, there are no experiments comparing the Raman signal of chemical species

[a]*Centro de Tecnologías Físicas, Unidad Asociada ICMM/CSIC-UPV, Universidad Politécnica de Valencia, Av. Los Naranjos s/n, Valencia, 46022, Spain*

[b]*Instituto de Ciencia de Materiales de Madrid, CSIC, Madrid, 28049, Spain. E-mail: fmese@fis.upv.es*

[c]*Department of Chemical Engineering, Texas Materials Institute, Center for Nano- and Molecular Science and Technology, The University of Texas at Austin, Austin, Texas 78712-1062, USA*

[d]*Departamento de Quimica Fisica e Inorganica, Universitat Rovira i Virgili and Centro de Tecnología Química de Catalunya, Carrer de Marcel lí Domingo s/n, 43007 Tarragona, Spain. E-mail: ramon.alvarez@urv.cat*

[e]*ICREA, Passeig Lluís Companys 23, 08010 Barcelona, Spain*

† Electronic supplementary information (ESI) available. See DOI: 10.1039/c4nr00593g

attached to either gold or high refractive index dielectric nanoparticles, like silicon. Silicon has several advantages over noble metals including low losses in the optical region, sharp wavelength Mie resonances strongly dependent on the particle size,[25,34] different surface chemistry, biocompatibility and biodegradability.[35]

In this communication we proved the concept for the Raman amplification of minute concentrations of organic species attached to the surface of silicon nanoparticles. Implications of this demonstration include the expansion of the number of organic families that can be sampled directly with SERS usually restricted to those carrying functional groups with high affinity for gold and silver, the decrease in the price of production of this materials and the possibility of using single particles of larger sizes for optical monitoring with SERS.

Raman amplification is obtained on molecules in close proximity to the optical enhancer surfaces. The enhancement factor is related to the evanescent field around the particles, which, in turn, is also related to their scattering cross-section values. The scattering cross-section depends on the topology of the silicon nanoparticle. Fig. 1 shows the scattering cross-section of spherical silicon nanoparticles as a function of the size parameter value, k, defined as $k = \pi d/\lambda$, where d and λ being the particle diameter and the light wavelength values, respectively.

The spectra shown in Fig. 1 is a well-known universal profile, which does not depend on the particle size, provided the refractive index is not dispersive and the material has a small absorption value.[23] We have chosen a conventional near infrared (NIR) Raman laser wavelength (785 nm) for the proof of concept of our results, since this wavelength value is located in the transparency region of biological tissue (650–900 nm),[36] and because silicon shows a small absorption value. Notably, and in contrast to gold nanoparticles, the wavelength position of the Mie resonances of silicon can be deeply tuned with the particle size.[25,34] Therefore, SiNPs may be suitable candidates for enhancing the Raman signal of the molecular species attached to them provided they are monodisperse. The calculation of the total evanescent field around the nanoparticles of different sizes when they are shined with the working laser line is shown in Fig. 2. The input parameters are the particle size and the refractive index value of silicon in the calculated wavelength region (see ESI†). In contrast to the gold case, SiNPs show narrow peaks at a large particle size corresponding to the high order Mie resonances and a broad structure at low values of the particle size coming from the low order modes resonances (see the peak description in Fig. 1 and 1S in the ESI†). These results show that the evanescent field of the silicon nanoparticles is, roughly speaking, smaller than that of the gold ones. However, at certain particle size values where Mie modes resonate with the laser line, the evanescent field around silicon will have the same or even larger level intensity than those for gold plasmons. Gold nanoparticles also show peaks at certain particles values, but the strong damping effects of gold attenuate the resonances.

The processing of monodisperse spherical nanoparticles with a strict control of the particle size is a challenging goal that has been achieved in restricted cases for a limited range of sizes.[37,38] However, the limited size values reported[37,38] do not allow tuning of the lowest size parameter value Mie resonances. Also the refractive index of porous particles[37] is not high enough for boosting the Raman signal at intensity levels similar to those obtained from SERS on gold NPs. The spherical topology, a necessary condition, for sustaining Mie resonances as well as the monodisperse quality of SiNPs can be relaxed for low index modes appearing at low size parameters (see Fig. 1). The broad resonances appearing in most of the Mie resonances of Fig. 1 permit using non-highly monodisperse silicon particles, provided the particles are non-porous and they have the refractive index value of bulk silicon. Also, their EM field map plot would be less sensitive to the surface topology of the nanocavities as the field map plots shown in Fig. 2, and also in the ESI.† Therefore as, at this stage, we cannot produce monodisperse spherical nanocavities with the appropriate

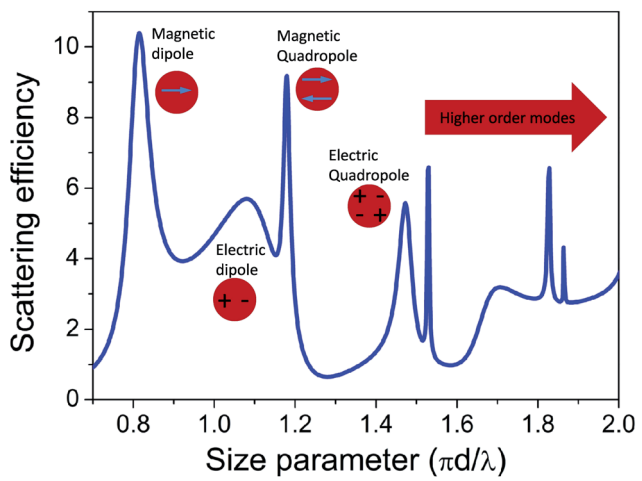

Fig. 1 Scattering efficiency of a single silicon spherical nanocavity as a function of the size parameter. We have assumed a constant value for the refractive index of silicon ($n = 3.7$).

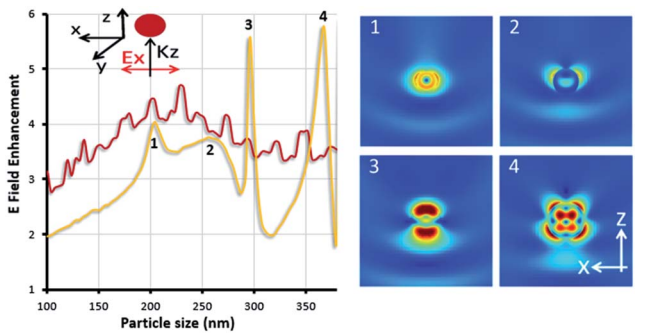

Fig. 2 Field enhancement around spherical particles of both silicon (yellow line) and gold (red line) as a function of the particle size when they are shined with a laser with a wavelength value of 785 nm, for particles embedded in air and the field distributions of the numbered peaks in the graph: (1) magnetic dipole, (2) electric dipole, (3) magnetic quadrupole, and (4) electric quadrupole modes.

particle diameter, we have processed monodisperse SiNPs with arbitrary surface topology with size values resonating at the four Mie resonances shown in Fig. 1 (see also Fig. 1S in the ESI†). The information reported below would give us information about the potentiality of SiNPs as SiPERS enhancers even in the case when they do not have a good spherical shape and good monodispersity values. We have processed silicon particles through mechanical milling of polycrystalline silicon. After several cycles of sedimentation,[39] we obtain monodisperse SiNPs with a refractive index value of bulk silicon (Fig. 3).

The separation process allows for the selection of monodisperse SiNPs with particle size values where the evanescence field calculation shows maxima and with a reasonable monodispersity value of 10%. Although the particles do not have a spherical shape, both the high refractive index value, as well as the topology of resonances involved, allow them to be used as SiPERS enhancers. In the following we will compare the Raman amplification signal from gold and silicon with the particle size values that maximizes their Raman signal.

To illustrate the Raman amplification efficiency and the surface composition of silicon and gold particles[40,41] on the SERS signal, samples were evaluated using *p*-aminobenzoic acid (PABA) as the probe molecule.

Both gold and silicon nanoparticles were illuminated with the near infrared laser (785 nm) as this laser line is conventional in many instruments. Also, it does not damage the sample as usually visible light does, and it is more appropriate for analysing biological samples as tissues are transparent to this radiation. As a first observation (Fig. 4a), the SERS intensity yielded by the gold nanoparticles show maximum values for particle size values around 100 nm. For increasing the particle size, the SERS signal decreases due to the increasing contribution of the radioactive damping, which is consistent with previous reports.[40] In the case of SiNPs, SiPERS signals of PABA were identified from sizes around 200, 260, 300 and 370 nm, which roughly correspond to the calculated particle size values where the laser line resonates (see peaks 1–4 in Fig. 2). It is worthy to note that for both cases spectral shapes remain stable from particle to particle while the intensity slightly fluctuates (see Fig. 4a) as commonly observed in this kind of experiments with a Raman amplification factor of 10^6, a usual value for isolated particles.

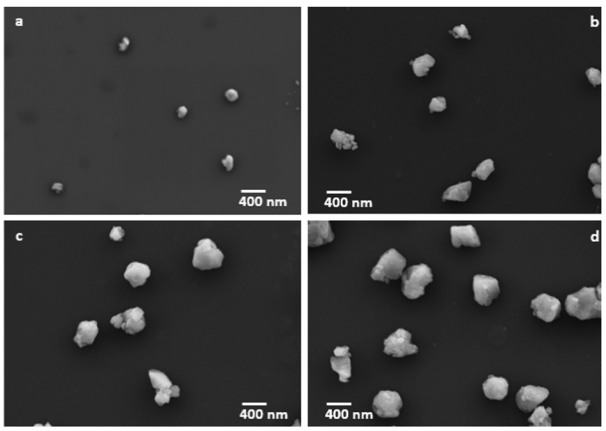

Fig. 3 SEM image of SiNPs obtained through mechanical milling of silicon powder together with further particle separation through a colloidal sedimentation process: (a) 200, (b) 260, (c) 300 and (d) 370 nm.

The calculation of the scattering cross-sections of silicon spherical particles as a function of the illumination wavelength (Fig. 1 and 1S in the ESI†) shows that these colloids exhibit several resonances at the low modal number Mie resonances, specifically magnetic dipole (Fig. 1Sa†), electric dipole (Fig. 1Sb†), magnetic quadrupole (Fig. 1Sc†) and electric quadrupole modes (Fig. 1Sd†) for sizes of 204, 256, 296 and 368 nm, respectively. Differences in the intensity are ascribed first not only to the increase of the near electric field generated by each mode, but also to the lower sphericity of the particles produced by mechanical milling. Notably, although in plasmonic particles the Raman amplification mainly relies on the electric fields generated by the electric dipolar plasmon resonances, in the case of silicon, fields are related to the higher order electric and magnetic Mie modes.[23,25]

SERS and SiPERS spectra of PABA also illustrate the effect of the surface chemistry of the particle on the Raman signal. PABA contains two different functionalities in the opposite parts of its aromatic ring, amino, and carboxylic acid groups. These groups show different affinity for each surface. While the amino group presents strong interactions with gold surfaces, carboxylic groups prefer silicon surfaces. SERS spectra of PABA as a function of optical enhancer are shown in the Fig. 4b. The SERS spectrum for gold is similar to those previously reported for PABA,[42] where the molecule is adsorbed through the amino group. The vibrational frequencies observed on the gold–PABA spectrum fit band to band with the Raman spectrum of the PABA in bulk. However, the relative intensities in the SERS spectrum show strong enhancement of the ν19a ring mode (1515 cm^{-1}) and the band corresponding to the rocking vibration of the amino group (983 cm^{-1}).[43] In fact, the increase in relative intensity of this band can be explained if the amino group is directly attached to the gold surface. Additionally, the band at 1700 cm^{-1} assigned to the C=O stretching is not visible in the Raman spectrum. The reason for the appearance of this band may be explained because of the complex formed between the amino group and gold. Gold colloids are strong electron-donors, thus, when the PABA is attached to them, the aromatic rings become electron acceptors, hindering the dissociation of the carboxylic group. The presence of ν(C=O) band strongly supports the hypothesis that the carboxylic group is not interacting with the surface. Notably, when SiPERS is carried out on the silicon colloids, the spectrum shows changes in the relative intensity of the bands. First, the band at 1515 cm^{-1} (ν19a) decreases while those at 1450 cm^{-1} (ν19b) increases indicating a change in the molecular orientation with respect to the surface. Further, and more importantly, the C=O stretching mode (1700 cm^{-1} band) disappears suggesting a direct interaction between the silicon surfaces and the carboxylic group. This hypothesis is also supported because of the emergence of a strong new band at 1542 cm^{-1} that could be assigned to the NH_2 asymmetric deformation.

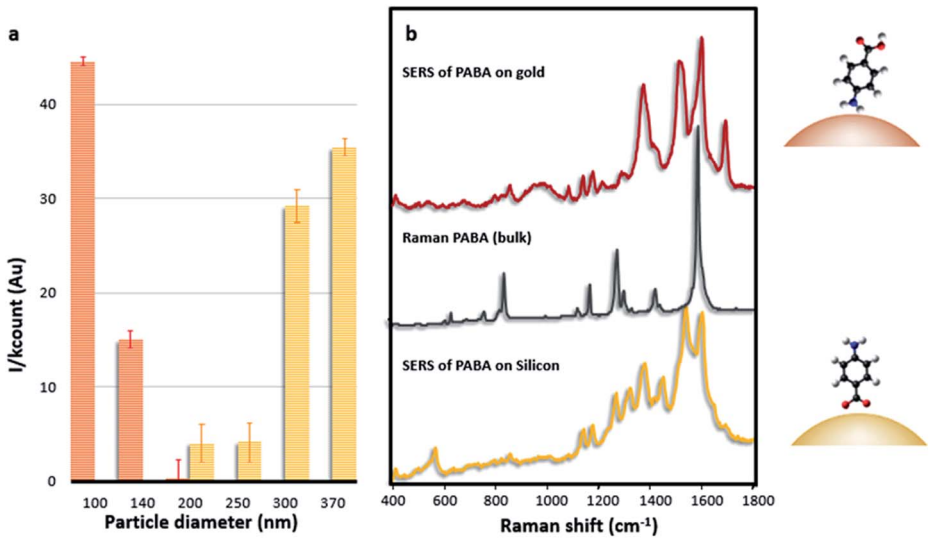

Fig. 4 (a) Intensities and (b) SERS spectra of PABA excited at 785 nm on colloidal dispersions of gold (100–400 nm) and silicon (200–370 nm) particles. Gold (red) and silicon (yellow).

Conclusions

To conclude herein we show the great potentiality of SiNPs as Raman signal enhancers of organic molecules attached to them and, induced by the huge evanescent fields associated with the Mie resonances of non-spherical shape nanoparticles. It may open the door for the generation of a new biocompatible, and biodegradable[35,44] surface for biosensing, easily attainable with standard particle processing techniques. Further, these new active optical surfaces show different affinities to the conventional plasmonic noble metals paving the road for the direct analysis of families of molecules difficult to detect with gold or silver due to their small affinity with such metals.

Acknowledgements

The authors acknowledge financial support from the following projects FIS2009-07812, MAT2012-35040, Consolider 2007-0046 Nanolight, PROMETEO/2010/043, CTQ2011-23167, and Cross-SERS, FP7 MC-IEF 329131. L. S. thanks the financial support from the MINECO (Estancias de profesores e investigadores extranjeros en centros españoles) fellowship program.

Notes and references

1 C. M. Soukoulis and M. Wegener, *Nat. Photonics*, 2011, **5**, 523.
2 W. Cai and V. Shalaev, *Optical Metamaterials: Fundamentals and Applications*, Springer, 2010.
3 R. Merlin, *Science*, 2007, **317**, 927.
4 P. L. Stiles, J. A. Dieringer, N. C. Shah and R. P. Van Duyne, *Annu. Rev. Anal. Chem.*, 2008, **1**, 601.
5 M. Moskovits, *Notes Rec. R. Soc.*, 2012, **66**, 195.
6 R. A. Alvarez-Puebla and L. M. Liz-Marzán, *Angew. Chem., Int. Ed.*, 2012, **51**, 11214.
7 R. S. Golightly, W. E. Doering and M. J. Natan, *ACS Nano*, 2009, **3**, 2859.
8 U. Kreibig and M. Vollmer, *Optical properties of metal clusters*, Springer, 1995.
9 N. J. Halas, S. Lal, W.-S. Chang, S. Link and P. Nordlander, *Chem. Rev.*, 2011, **111**, 3913.
10 L. Rodriguez-Lorenzo, R. A. Alvarez-Puebla, I. Pastoriza-Santos, S. Mazzucco, O. Stephan, M. Kociak, L. M. Liz-Marzan and F. J. Garcia de Abajo, *J. Am. Chem. Soc.*, 2009, **131**, 4616.
11 E. Cortés, P. G. Etchegoin, E. C. Le Ru, A. Fainstein, M. E. Vela and R. C. Salvarezza, *J. Am. Chem. Soc.*, 2013, **135**, 2809.
12 N. P. W. Pieczonka and R. F. Aroca, *Chem. Soc. Rev.*, 2008, **37**, 946.
13 M. W. Knight, L. Liu, Y. Wang, L. Brown, S. Mukherjee, N. S. King, H. O. Everitt, P. Nordlander and N. J. Halas, *Nano Lett.*, 2012, **12**, 6000.
14 L. Li, T. Hutter, A. S. Finnemore, F. M. Huang, J. J. Baumberg, S. R. Elliott, U. Steiner and S. Mahajan, *Nano Lett.*, 2012, **12**, 4242.
15 W. Li, R. Zamani, P. Rivera-Gil, B. Pelaz, M. Ibáñez, D. Cadavid, A. Shavel, R. A. Alvarez-Puebla, W. J. Parak, J. Arbiol and A. Cabot, *J. Am. Chem. Soc.*, 2013, **135**, 7098.
16 D. J. Rowe, J. S. Jeong, K. A. Mkhoyan and U. R. Kortshagen, *Nano Lett.*, 2013, **13**, 1317.
17 Y. Wang, J. Zhang, H. Jia, M. Li, J. Zeng, B. Yang, B. Zhao, W. Xu and J. R. Lombardi, *J. Phys. Chem. C*, 2008, **112**, 996.
18 M. Begliarbekov, O. Sul, J. Santanello, N. Ai, X. Zhang, E. H. Yang and S. Strauf, *Nano Lett.*, 2011, **11**, 1254.
19 X. Ling, L. Xie, Y. Fang, H. Xu, H. Zhang, J. Kong, M. S. Dresselhaus, J. Zhang and Z. Liu, *Nano Lett.*, 2009, **10**, 553.
20 E. S. Thrall, A. C. Crowther, Z. Yu and L. E. Brus, *Nano Lett.*, 2012, **12**, 1571.

21 A. Delfan, M. Liscidini and J. E. Sipe, *J. Opt. Soc. Am. B*, 2012, **29**, 1863.
22 S. Pirotta, X. G. Xu, A. Delfan, S. Mysore, S. Maiti, G. Dacarro, M. Patrini, M. Galli, G. Guizzetti, D. Bajoni, J. E. Sipe, G. C. Walker and M. Liscidini, *J. Phys. Chem. C*, 2013, **117**, 6821.
23 C. F. Bohren and D. R. Huffman, *Absorption and scattering of light by small particles*, Wiley, 1983.
24 J. D. Eversole, H.-B. Lin, A. L. Huston and A. J. Campillo, *J. Opt. Soc. Am. A*, 1990, **7**, 2159.
25 L. Shi, T. U. Tuzer, R. Fenollosa and F. Meseguer, *Adv. Mater.*, 2012, **24**, 5934.
26 D. V. Murphy and S. R. J. Brueck, *Opt. Lett.*, 1983, **8**, 494.
27 J. B. Snow, S.-X. Qian and R. K. Chang, *Opt. Lett.*, 1985, **10**, 37.
28 R. Symes, R. M. Sayer and J. P. Reid, *Phys. Chem. Chem. Phys.*, 2004, **6**, 474.
29 R. J. Hopkins and J. P. Reid, *J. Phys. Chem. B*, 2006, **110**, 3239.
30 L. K. Ausman and G. C. Schatz, *J. Chem. Phys.*, 2008, **129**, 054704.
31 M. S. Andersson, *Appl. Phys. Lett.*, 2010, **97**, 131116.
32 I. Alessandri, *J. Am. Chem. Soc.*, 2013, **135**, 5541.
33 S. M. Wells, I. A. Merkulov, I. I. Kravchenko, N. V. Lavrik and M. J. Sepaniak, *ACS Nano*, 2012, **6**, 2948.
34 E. Xifré-Pérez, R. Fenollosa and F. Meseguer, *Opt. Express*, 2011, **19**, 3455.
35 L. T. Canham, *Adv. Mater.*, 1995, **7**, 1033.
36 R. Weissleder, *Nat. Biotechnol.*, 2001, **19**, 321.
37 L. Shi, J. T. Harris, R. Fenollosa, I. Rodriguez, X. Lu, B. A. Korgel and F. Meseguer, *Nat. Commun.*, 2013, **4**, 1904.
38 A. Gumennik, L. Wei, G. Lestoquoy, A. M. Stolyarov, X. Jia, P. H. Rekemeyer, M. J. Smith, X. Lianf, B. J.-B. Grena, S. G. Johnson, S. Gradecak, A. F. Abouraddy, J. D. Joannopoulos and Y. Fink, *Nat. Commun.*, 2013, **4**, 2216.
39 I. Rodriguez, R. Fenollosa, F. Meseguer and A. Perez-Roldan, ES 2386126, WO 2012101306, 2011.
40 N. Pazos-Perez, F. J. Garcia de Abajo, A. Fery and R. A. Alvarez-Puebla, *Langmuir*, 2012, **28**, 8909.
41 N. G. Bastús, J. Comenge and V. Puntes, *Langmuir*, 2011, **27**, 11098.
42 S. Sánchez-Cortés, J. V. Garcia-Ramos and G. Morcillo, *J. Colloid Interface Sci.*, 1994, **167**, 428.
43 H. Park, S. B. Lee, K. Kim and M. S. J. Kim, *Phys. Chem.*, 1990, **94**, 7576.
44 J. H. Park, L. Gu, G. von Maltzahn, E. Ruoslahti, S. N. Bhatia and M. J. Sailor, *Nat. Mater.*, 2009, **8**, 331.